

Supporting information for:

## Modular and Chemically Responsive Oligonucleotide “Bonds” in Nanoparticle Superlattices

Stacey N. Barnaby, Ryan V. Thaner, Michael B. Ross, Keith A. Brown<sup>‡</sup>, George C. Schatz, and Chad A. Mirkin\*

Department of Chemistry and International Institute for Nanotechnology, Northwestern University, 2145 Sheridan Road, Evanston, IL 60208, United States.

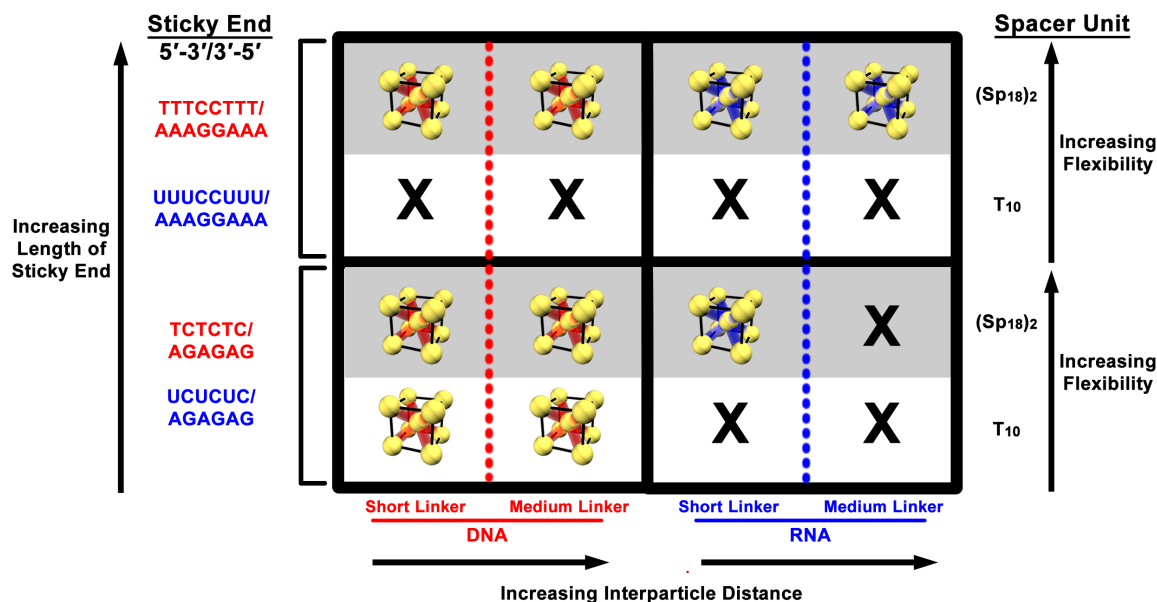
<sup>‡</sup>Current address: Department of Mechanical Engineering, Boston University, 110 Cummington Mall, Boston, MA 02215, United States.

\*Correspondence: [chadnano@northwestern.edu](mailto:chadnano@northwestern.edu)

Thiol Modified Oligonucleotides	Sequence (5' → 3')
DNA A	AAC AAT TAT ACT CAG CAA (Sp18) <sub>2</sub> SH
DNA B	TAT CGT ATT TAC TCT GAT (Sp18) <sub>2</sub> SH
RNA A	rArArC rArArU rUrArU rArCrU rCrArG rCrArA (Sp18) <sub>2</sub> SH
RNA B	rUrArU rCrGrU rArUrU rUrACr rUrCrU rGrArU (Sp18) <sub>2</sub> SH
Linker Oligonucleotides	Sequence (5' → 3')
AuNP Recognition DNA A	TTG CTG AGT ATA ATT GTT ...
Short DNA A	... A TTTCTTT
Medium DNA A	... A TTT AGT CAC GAC GAG TCA TT A TTTCTTT
Long DNA A	... A TTT AGT CAC GAC GAG TCA TT TTT AGT CAC GAC GAG TCA TT A TTTCTTT
AuNP Recognition DNA B	ATC AGA GTA AAT ACG ATA ...
Short DNA B	... A AAAGGAAA
Medium DNA B	... A TTT AGT CAC GAC GAG TCA TT A AAAGGAAA
Long DNA B	... A TTT AGT CAC GAC GAG TCA TT TTT AGT CAC GAC GAG TCA TT A AAAGGAAA
AuNP Recognition RNA A	rUrUrG rCrUrG rArGrU rArUrA rArUrU rGrUrU ...
Short RNA A	... rA rUrUrUrCrUrUrU
Medium RNA A	... rA rUrUrU rArGrU rCrArC rGrArC rGrArG rUrCrA rUrU rA rUrUrUrCrUrUrU
Long RNA A	... rA rUrUrU rArGrU rCrArC rGrArC rGrArG rUrCrA rUrU rUrUrU rArGrU rCrArC rGrArC rGrArG rUrCrA rUrU rUrUrUrCrUrUrU
AuNP Recognition RNA B	rArUrC rArGrA rGrUrA rArArU rArCrG rArUrA ...
Short RNA B	... rA rArArGrGrArArA
Medium RNA B	... rA rUrUrU rArGrU rCrArC rGrArC rGrArG rUrCrA rUrU rA rArArGrGrArArA
Long RNA B	... rA rUrUrU rArGrU rCrArC rGrArC rGrArG rUrCrA rUrU rUrUrU rArGrU rCrArC rGrArC rGrArG rUrCrA rUrU rA rArArGrGrArArA
Duplexer Oligonucleotides	Sequence (5' → 3')
Medium DNA Duplexer	AAA TCA GTG CTG CTC AGT AA
Long DNA Duplexer	AA TGA CTC GTC GTG ACT AA AAA TGA CTC GTC GTG ACT AAA
Medium RNA Duplexer	rArArU rGrArC rUrCrG rUrCrG rUrGrA rCrUrA rArA
Long RNA Duplexer	rArA rUrGrA rCrUrC rGrUrC rGrUrG rArCrU rArA rArArA rUrGrA rCrUrC rGrUrC rGrUrG rArCrU rArArA

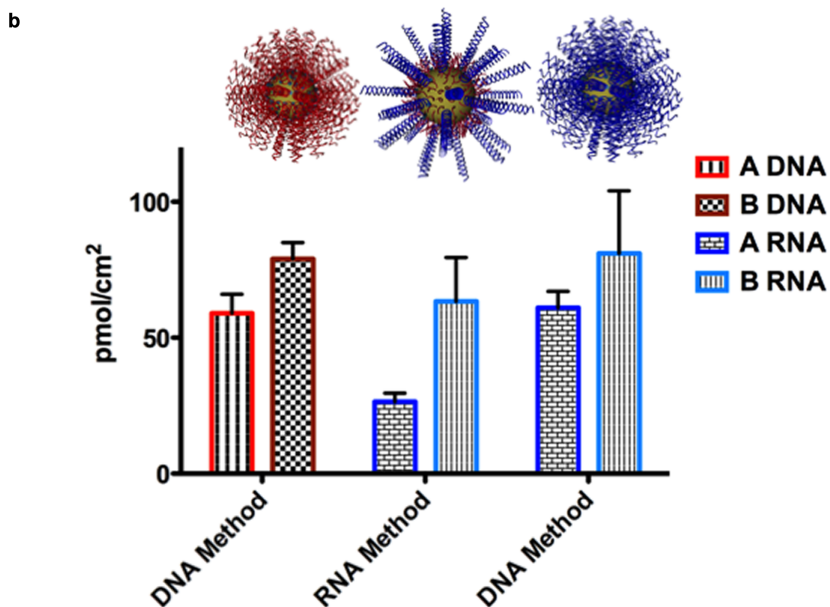
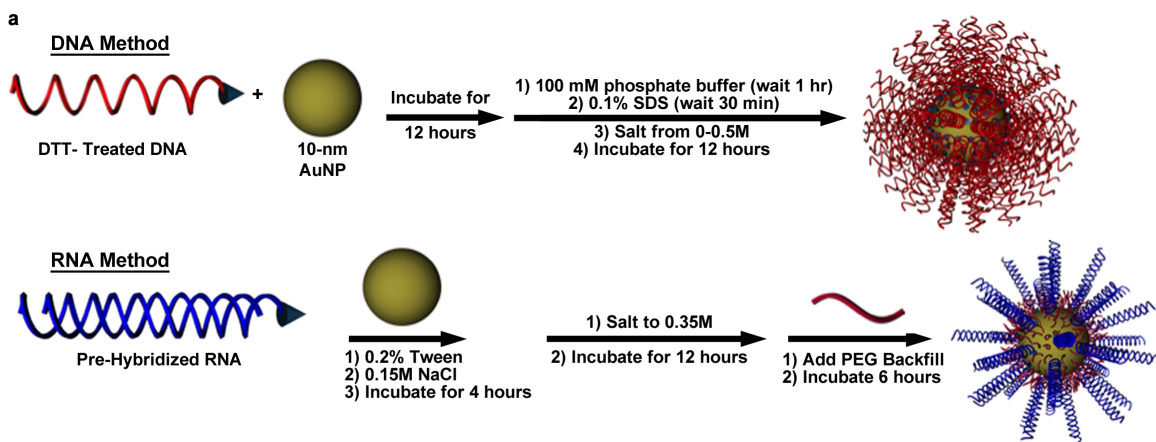
Note: (Sp18)<sub>2</sub> SH = HS-C<sub>3</sub>H<sub>6</sub>-O-[(C<sub>2</sub>H<sub>4</sub>O)<sub>6</sub>-PO<sub>3</sub>]<sub>2</sub>

Table S1. Oligonucleotide Sequences.



**Figure S1.** Exploring Design Space to Assemble bcc Nanoparticle Superlattices.

Design rules exist for the synthesis of nanoparticle superlattices using DNA as a programmable ligand.<sup>1</sup> In order to synthesize nanoparticle superlattices using RNA as a programmable ligand, the sticky end strength (left) and spacer unit (right) were used to toggle the strength of the interaction and the flexibility of the linker respectively (sequences in Table S1). Two different linkers (left) were explored to modulate the length between the nanoparticles (bottom). For the long sticky end (TTCCTTT/AAAGGAAA for DNA and UUCCUUU/AAAGGAAA for RNA) with the flexible spacer ( $(Sp_{18})_2$ ), ordered crystals resulted in all case (top row) whereas for the long sticky end with the rigid spacer unit (second row from top), only amorphous aggregates were observed (indicated by X). Therefore, all crystals assembled herein utilize a strong sticky end with a flexible spacer. The  $T_{10}$  spacer is a DNA spacer with 10 thymine nucleobases and  $(Sp_{18})_2$  is the same polyethylene glycol (PEG) spacer defined in Table S1.



**Figure S2.** Synthesis of Programmable Atom Equivalent (PAE) Building Blocks and Quantification of Oligonucleotides.

- Synthesis of particle A and particle B using two different methods (sequences in Table S1). The PAEs prepared *via* the “DNA Method”<sup>1</sup> and “RNA Method”<sup>2</sup> were synthesized by modification of previous methods. The backfill utilized was 10  $\mu$ M of 2 kDa polyethylene glycol (PEG; Nanocs). DTT stands for dithiothreitol. Detailed experimental details can be found in the SI Materials and Methods.
- Comparable oligonucleotide loading was achieved for both thiolated DNA and RNA using the “DNA Method”, where particle A has a density of 55 pmol/cm<sup>2</sup> and particle B has a density of 80 pmol/cm<sup>2</sup>. This was achieved by preparing the RNA version of particle A and particle B using the same method used to prepare the DNA version of particle A and particle B. Previous studies have reported the synthesis of AuNPs functionalized with double stranded RNA and backfilled with either oligoethylene glycol<sup>3</sup> or short PEG<sup>2</sup>, where it was reported that there are about 30 small interfering RNA (siRNA) duplexes on 13-nm AuNPs and 100 single-stranded

RNA (ssRNA) oligonucleotides for a density of about 25 pmol/cm<sup>2</sup> for the thiolated ssRNA oligonucleotide, which is similar to what we observed for particle A and B synthesized by the “RNA Method”. Not only is the surface chemistry of these particles different than those prepared by the “DNA Method” because they are passivated with a polymer, but the density of ssRNA is substantially lower than for ssDNA, where an oligonucleotide density of 56 pmol/cm<sup>2</sup> was reported for a similar particle (different sequence) functionalized with DNA.<sup>4</sup> Therefore, synthesis of RNA particles A and B using the “DNA Method” nearly doubles the thiolated oligonucleotide density on AuNP surfaces and is essential for utilizing RNA as the programmable ligand. Error bars represent N=4 measurements of oligonucleotide density on independently synthesized PAEs.

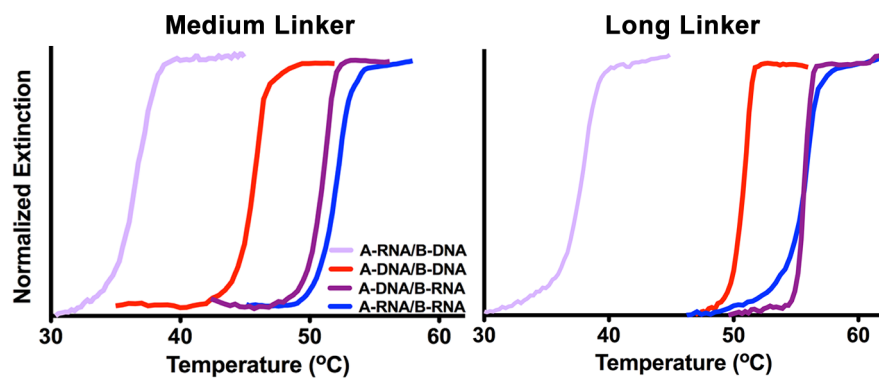


**Figure S3.** Melting Transitions of Nanoparticle Superlattices. Melting curves for nanoparticle superlattices of medium (left) and long (right) linker lengths. The same trend emerges for increasing melting temperature regardless of linker length: A-RNA/B-DNA (light purple), A-DNA/B-DNA (red), A-DNA/B-RNA (dark purple), and then A-RNA/B-RNA (blue). Detailed experimental procedure can be found in the Materials and Methods.

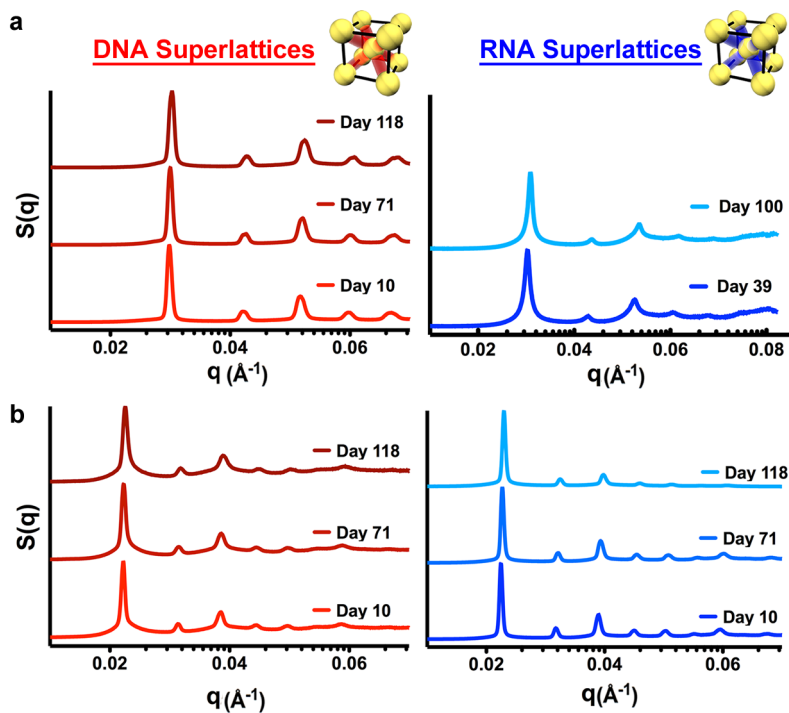


**Figure S4.** Stability of Nanoparticle Superlattices Over Time. Superlattices were slowly cooled and then loaded into quartz capillary tubes. Day 1 denotes the day at which particles A and B were mixed in equimolar ratios. The slow-cooled nanoparticle superlattices of small (a) and medium (b) linker lengths were analyzed by small angle X-ray scattering (SAXS) on the days indicated above. At all times, superlattices were stored at room temperature and protected from light. These data demonstrate suitable stability of RNA for use as a programmable ligand.

Linker Length (bp)	# of Days Post Assembly	Interparticle Distance	Crystal Domain Size
<b>46</b>	<b>10</b>	<b>25.80 nm</b>	<b>690 nm</b>
	<b>71</b>	<b>25.66 nm</b>	<b>690 nm</b>
	<b>118</b>	<b>25.41 nm</b>	<b>680 nm</b>
<b>67</b>	<b>10</b>	<b>34.63 nm</b>	<b>930 nm</b>
	<b>71</b>	<b>34.47 nm</b>	<b>925 nm</b>
	<b>118</b>	<b>34.08 nm</b>	<b>915 nm</b>
<b>46</b>	<b>39</b>	<b>25.39 nm</b>	<b>680 nm</b>
	<b>100</b>	<b>24.92 nm</b>	<b>670 nm</b>
<b>67</b>	<b>10</b>	<b>34.22 nm</b>	<b>920 nm</b>
	<b>71</b>	<b>33.91 nm</b>	<b>910 nm</b>
	<b>118</b>	<b>33.45 nm</b>	<b>900 nm</b>

**Table S2.** Interparticle Distance and Crystal Domain Size for Nanoparticle Superlattices Over Time. The interparticle distance and crystal domain were calculated from the SAXS data in Figure S2 using the equations described in the Materials and Methods.

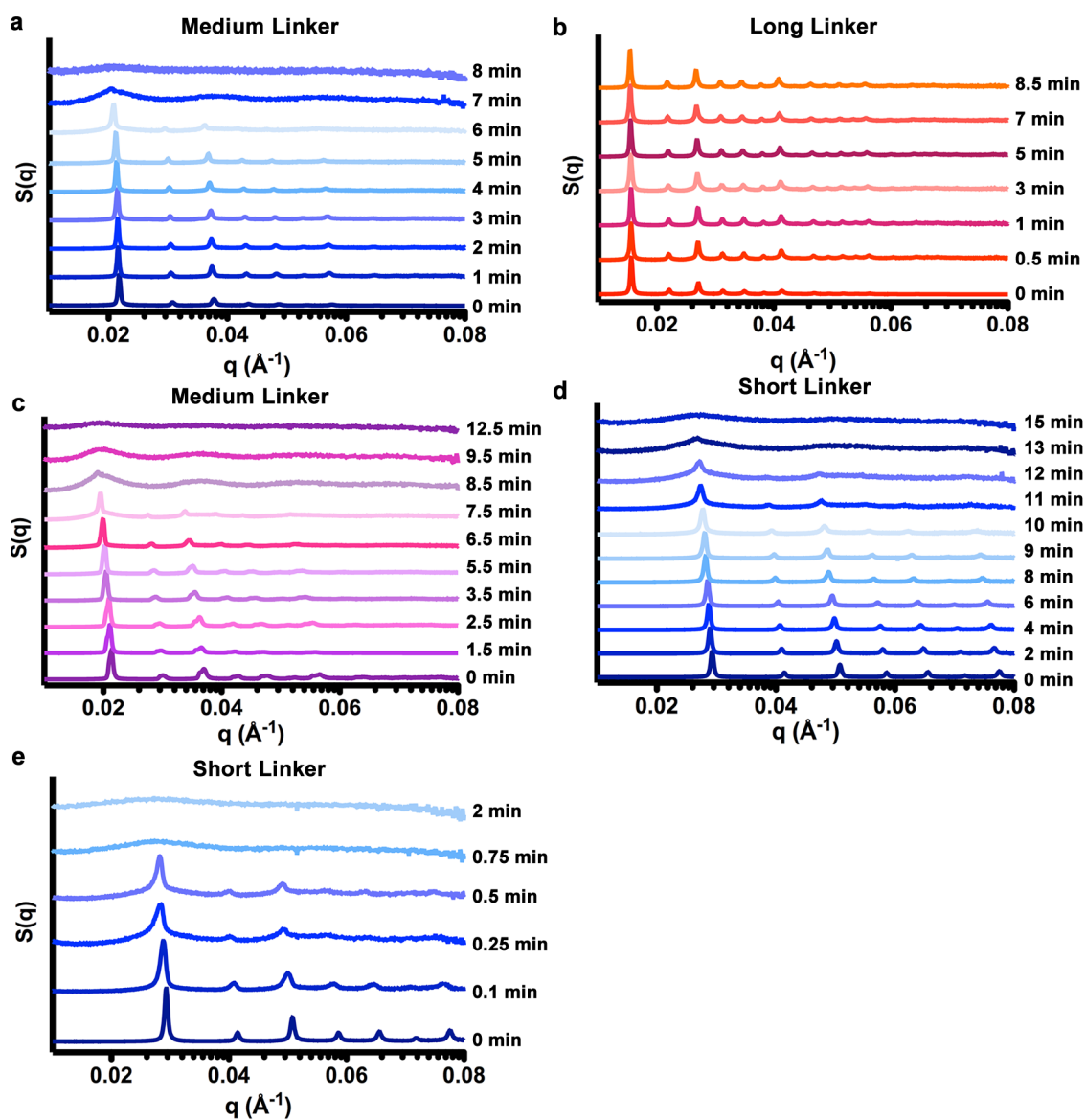


**Figure S5.** Time-Dependent SAXS for Nanoparticle Superlattices with Ribonuclease (RNase) A. Experiments were performed using a flow cell, where enzymes were flowed over a suspension of nanoparticle superlattices and SAXS scattering patterns were taken at the time points designated above. Detailed experimental description is provided in the Materials and Methods. All experiments were performed at 37 °C. [AuNP]  $\approx$  45 nM

- RNA superlattices with medium linkers upon incubation with 1  $\mu$ g RNase A.
- DNA superlattices with long linkers upon incubation with 1  $\mu$ g RNase A.
- Hybrid superlattices with medium linkers upon incubation with 1  $\mu$ g RNase A.
- RNA superlattices with medium linkers upon incubation with 0.5  $\mu$ g RNase A.
- RNA superlattices with medium linkers upon incubation with 6  $\mu$ g RNase A.



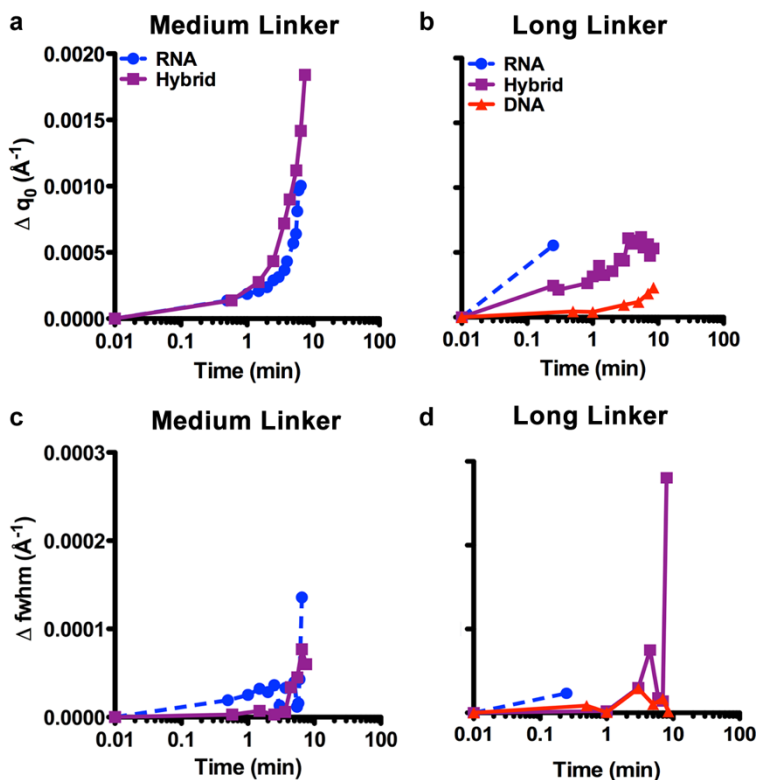


**Figure S6.** Measurement of the Superlattice Response to Enzymes.

- Changes in the position of the first order scattering peak ( $\Delta q_0$ ) over time extracted from the time-dependent SAXS data for RNA (blue circles) and hybrid (purple squares) nanoparticle superlattices with medium linkers. The magnitude of  $\Delta q_0$  and the time over which this transition occurs are both greater for the hybrid superlattices as they retain their ordering of a greater period of time. Data was analyzed from time-dependent SAXS data until long-range order was no longer preserved (6 min for RNA and 7.5 min for hybrid superlattices).
- $\Delta q_0$  over time extracted from the time-dependent SAXS data for RNA, hybrid, and DNA nanoparticle superlattices with long linkers. The interparticle distance increases for all nanoparticle superlattices but the magnitude and time over which this increase occurs is dependant on oligonucleotide bond composition.
- Changes in the fwhm ( $\Delta \text{fwhm}$ ) of the first order scattering peak as a function of time. The quality of the crystal is maintained longer for the hybrid nanoparticle superlattice than the RNA superlattice. Data was analyzed from time-dependent SAXS data until long-range order was no longer preserved (0.25 min for RNA and 8.5 min for hybrid superlattices).
- $\Delta \text{fwhm}$  of the first order scattering peak as a function of time. Almost no change in crystal quality is seen for the DNA nanoparticle superlattice over 10 minutes, whereas the hybrid nanoparticle superlattice begins to decrease in quality at 8.5 minutes. The RNA superlattice is completely disordered at 30 s and thus only a small decrease in quality is observed.

Oligonucleotide	Linker Length (Total)	T <sub>m</sub>	Slow Cool Parameters
DNA	46	49	55 °C to 25 °C
DNA	67	50	55 °C to 25 °C
DNA	128	49	55 °C to 25 °C
A DNA- B RNA	46	56	60 °C to 25 °C
A DNA- B RNA	67	55	60 °C to 25 °C
A DNA- B RNA	128	56	60 °C to 25 °C
A RNA- B DNA	46	36	45 °C to 25 °C
A RNA- B DNA	67	35	45 °C to 25 °C
A RNA- B DNA	128	38	45 °C to 25 °C
RNA	46	59	60 °C to 25 °C
RNA	67	55	60 °C to 25 °C
RNA	128	55	60 °C to 25 °C

**Table S3.** Melting Temperatures and Slow Cool Parameters. The melting temperatures were obtained from UV-vis melting analyses of all nanoparticle aggregates. The slow cool annealing temperature parameters were based off the result of the UV-vis melting analyses. The protocol for obtaining the melting curves and running the slow cool annealing are explained in detail in the Materials and Methods.

## **Materials and Methods**

### **Preparation of Sterile, RNase-Free Solutions**

To prepare sterile solutions of water, 1x phosphate buffered saline (PBS; Corning), and 5 M sodium chloride (NaCl; Sigma-Aldrich), 1 mL of diethylprocarbonate (DEPC; Sigma-Aldrich) was added to 1 L of the aforementioned solution. The mixture was then shaken at 50 rpm for 2 h at 45 °C before being autoclaved.

### **Synthesis of DNA and RNA Oligonucleotides**

DNA oligonucleotides were synthesized on an MM48 DNA synthesizer (BioAutomation) with reagents obtained from Glen Research or ChemGenes. RNA oligonucleotides were synthesized using 2'-O [(trisopropylsilyl)oxy] methyl-RNA phosphoramidites (ChemGenes) on a MerMade 12 system (Bioautomation) according to the manufacturer-recommended cleavage and deprotection protocols. All oligonucleotides were purified using reverse-phase high-performance liquid chromatography (RP-HPLC) on a Varian Microsorb C18 column (10  $\mu$ M; 300 Å~ 10 mm) with 0.1 M triethylammonium acetate (TEAA) at pH 7 with a 1% gradient of 100% CH<sub>3</sub>CN at a flow rate of 3 mL/min, while monitoring the UV signal of the nucleic acids at 254 nm. After purification, the oligonucleotides were lyophilized, resuspended in sterile water, and stored at -80 °C.

### **Functionalization of Nanoparticles with DNA (The “DNA Method”)**

10-nm gold nanoparticles (AuNPs) were purchased from Ted Pella and used as received. DNA and RNA functionalization was conducted according to modified literature procedures for functionalization of DNA.<sup>4,5</sup> Briefly, oligonucleotides synthesized with a propyl-thiol modified 3' terminus were treated with 100 mM dithiothreitol (DTT; Sigma-Aldrich) for one hour at room temperature to reduce the disulfide, at which point the DTT

was removed *via* size-exclusion chromatography with a NAP5 or NAP10 column (GE Healthcare). The concentration of the oligonucleotides was confirmed using a NanoDrop1000 (ThermoScientific) and then added to gold nanoparticle suspensions at a ratio of 1 optical density (OD) unit of DNA or RNA per 1 mL of AuNPs (approximately 3 nmol of DNA or RNA per 1 mL of AuNPs) and placed on a rotary shaker (Sigma Aldrich). After incubation for 2- 12 hours, the solution was brought to 100 mM phosphate buffer (pH = 7.4) and left on a rotary shaker for 1 hour, at which point the solution was brought to 0.1% sodium dodecyl sulfate (SDS; Ambion) and left on the rotary shaker for an additional 30 min. The solution was slowly salted from 0- 0.5 M NaCl using a stock solution of 5 M NaCl, where the salt was raised 0.05- 0.1 M every 30 min. Once the solution was at 0.5 M NaCl, it was placed on the rotary shaker for 12 hours. Excess DNA or RNA was removed *via* centrifugation using Amicon Ultra-15 centrifugal filter unit (50-kDa cutoff; EMD Millipore) for 10 min in a swinging bucket rotor at 1,500 x g. The flow-through was removed and the particles were washed four times with 0.01% Tween-20 (Sigma Aldrich) in 1x PBS and centrifuged in an Eppendorf tube for 90 min at 21,000 x g. The supernatant was removed and the pellet was resuspended in 0.5 M NaCl. The AuNP concentration was measured by absorbance at 520 nm ( $E_{520\text{nm}} = 9.55 \times 10^8 \text{ M}^{-1} \text{ cm}^{-1}$ ) using a Cary 5000 UV-Vis. The SNAs were stored at 4-25 °C when not in use.

### **Functionalization of Nanoparticles with RNA (The “RNA Method”)**

To duplex RNA, the thiolated RNA oligonucleotide and the short RNA linker were hybridized in a buffer consisting of 30 mM HEPES (4-(2-hydroxyethyl)-1-piperazineethanesulfonic acid) and 100 mM potassium acetate, pH 7.5 (available from IDT) by first heating the solution to 95 °C for 10 min, then cooling to 37 °C for 60 min

while shaking at 350 rpm in a thermomixer (Benchmark Scientific). Duplexed RNA was added to solutions of 10-nm AuNPs in 0.2% Tween-20 (vol/vol) and 150 mM NaCl (final RNA concentration = 2  $\mu$ M). The solution was then sonicated for 30 s and placed on a rotary shaker for 4 hours, at which point the NaCl concentration was increased to 350 mM and allowed to shake for 16 hours. The solution was then brought to 10  $\mu$ M in thiolated 2 kDa polyethylene glycol (PEG; Nanocs) and allowed to shake for 4 hours. Purification was then performed in the same manner as described above. The SNAs were stored at 4 °C when not in use.

### **Measurement of the Surface Density of Thiolated Oligonucleotides per AuNP**

To measure the ratio of oligonucleotides per AuNP, Quant-iT OliGreen (Invitrogen) assays against a standard curve were performed by modification of previously established methods.<sup>2</sup> Briefly, 100  $\mu$ L of 2 nM AuNPs functionalized with A or B DNA or RNA was added to 100  $\mu$ L of 40 mM potassium cyanide (KCN) and heated at 55 °C for 10 min to release the oligonucleotides from the solution of the AuNPs through the formation of the water-soluble salt potassium gold cyanide. A portion of the solution (25  $\mu$ L) was analyzed by mixing with OliGreen reagent and measurement of the OliGreen fluorescence ( $\lambda_{\text{ex}}$  = 480 nm; Biotek synergy plate reader) in a 96-well plate (Denville Scientific).

### **Preparation of Programmable Atom Equivalents (PAEs)**

To prepare PAEs, hybridization of linker strands that present short sticky ends at the periphery of the particles' hydrodynamic radii of DNA and RNA must occur onto the thiol- oligonucleotide functionalized AuNPs. For the medium and long linkers, a duplex strand must first be added to the respective medium and long linkers (sequences in Table S1). To prepare the medium and long linkers, the RNA and DNA linker strands are first

combined with the complementary duplex strand. The linkers were then allowed to hybridize for  $\geq 1$  hour while shaking at 37 °C in a thermomixer to facilitate the formation of double stranded DNA- and RNA duplexes consisting of the oligonucleotide linker and its complementary sequence (duplex). The duplexed linkers (as well as the non-duplexed short linkers) were added to the AuNPs at 120 equivalents (relative to the number of moles of Au). The AuNPs with their linkers were allowed to hybridize for  $\geq 1$  hour while shaking at 37 °C in a thermomixer to form PAEs. Particle A and particle B, in all combinations of DNA-DNA, DNA-RNA, RNA-DNA, and RNA-RNA, were mixed in equimolar ratios and allowed to sit at room temperature for 1-2 hours to allow the particles to aggregate and precipitate out of solution.

### **Melting Experiments**

Melting curves were measured with a Cary 5000 UV-Vis-NIR spectrophotometer (Agilent; Santa Clara, CA) equipped with a multicell holder with thermal control. Each sample was prepared by transferring 30  $\mu\text{L}$  of aggregates to 900  $\mu\text{L}$  of 0.5 M NaCl in an absorbance cuvette (Hellma Cells Inc.). While stirring, the temperature was increased from 25 °C to 70 °C at a rate of 0.2 °C/min while monitoring the extinction of the solution at 260 and 520 nm with the same data collection interval. As the temperature increased, the aggregates broke apart due to the dehybridization of the oligonucleotide duplexes formed between the sticky ends of adjacent, complementary particles. The resulting free particles no longer have dampened optical signals as when aggregated, which leads to an increase in the extinction at 260 and 520 nm, allowing for a determination of the melting temperature by taking the first derivative of the melting curve and finding the maximum value.

### **Slow-Cool Annealing of Nanoparticle Superlattices**

100  $\mu\text{L}$  of dispersed superlattices were transferred to 200  $\mu\text{L}$  polymerase chain reaction (PCR) strip tubes (Eppendorf). The samples were brought to a temperature 5-10  $^{\circ}\text{C}$  above their melting temperature and then slowly cooled to 25  $^{\circ}\text{C}$  at a rate of 0.01  $^{\circ}\text{C}/\text{min}$  using a ProFlex<sup>TM</sup> PCR system (Applied Biosystems). Depending on the starting temperature, the slow cooling took 1-3 days to complete. A list of superlattices, melting temperatures, and annealing parameters can be found in Table S3.

### **Small Angle X-Ray Scattering (SAXS)**

All synchrotron SAXS experiments were conducted at the Dow-Northwestern-Dupont Collaborative Access Team (DND-CAT) Beamline 5ID-D at the Advanced Photon Source (APS) at Argonne National Laboratory. Experiments were collected with 10 keV (wavelength  $\lambda = 1.24 \text{ \AA}$ ) collimated X-rays calibrated against a silver behenate standard. Exposure times of 0.1 and 1 second were used. Approximately 30  $\mu\text{L}$  of slow-cooled nanoparticle superlattices were loaded into 1.5 mm quartz capillary tubes (Charles Supper) and placed into a sample stage in the path of the X-ray beam. Two-dimensional scattering data were collected on a CCD area detector and converted to 1D data by taking a radial average of the 2D data to generate plots of scattering intensity  $I(q)$  as a function of the scattering vector  $q$  ( $q = 4\pi\sin\theta/\lambda$ , where  $\theta$  and  $\lambda$  are the scattering angle and wavelength of the X-rays used, respectively). The particle form factor,  $P(q)$ , the scattering due to individual dispersed particles in solution, was subtracted from the experimental data to obtain the lattice structure factor,  $S(q)$ . Form factor subtraction, radial averaging, and other SAXS data analysis were performed in Igor using the Irena and Nika macros (available free of charge from the APS at [usaxs.xray.aps.anl.gov/staff/ilavsky/irena.html](http://usaxs.xray.aps.anl.gov/staff/ilavsky/irena.html)).

### Calculation of Interparticle Distance from the SAXS data

The nearest neighbor distance,  $d$ , between particles in a superlattice can be calculated from the position of the first scattering peak,  $q_0$ , in the scattering pattern using the following relationship for bcc crystallographic symmetry:

$$\frac{d_{au}(nm)}{q_0} = 0.1 \cdot \sqrt{6} \cdot \pi \quad (1)$$

### Calculation of the Domain Size from the SAXS Data

The crystal domain size was calculated using the Scherrer formula:

$$t = \frac{0.9\lambda}{\beta \cos \theta} \quad (2)$$

where  $\lambda$  = the wavelength of scattered X-rays,  $\theta$  = the diffraction angle associated with the  $q_0$  peak, and  $\beta$  = the angular full width at half maximum of the  $q_0$  peak.

### Time-Dependent SAXS

Time-dependent SAXS experiments were conducted using a flow- cell setup at 37 °C. To obtain a baseline reading, SAXS patterns were first collected for 80  $\mu$ L of nanoparticle superlattices. After the collection, the superlattices were then dispensed into an Eppendorf tube, which contained 10  $\mu$ L of ribonuclease (RNase) A at desired concentrations. At this point, a 5  $\mu$ L air bubble was pulled into the system, followed by 80  $\mu$ L of sample, and then another 5  $\mu$ L air bubble. Once the hutch was closed, oscillation of the sample between the two air bubbles at 10  $\mu$ L/second began in order to allow the sample to mix. The sample was then shot with the X-ray beam approximately every 30 s. For all time-resolved measurements, the exposure time was 0.5 s. All tubing was rinsed with Nanopure water in between each run.



## **Analysis of Time-Resolved SAXS Data**

The position ( $q$ ) and the full-width at half-maximum (FWHM;  $\beta$ ) of the first order scattering peak ( $q_0$ ) were determined using a non-linear least squares fitting algorithm implemented in MATLAB. The first order peak was fit to a Pseudo-Voigt function (*i.e.* a linear combination of Gaussian and Lorentzian curves with the same FWHM) on a linear background. The choice of fitting to a Pseudo-Voigt function was motivated by large residuals present when fitting to just Gaussian or Lorentzian curves.

To plot the data in Fig. 4a and Fig. S6a, a subtraction was performed such that the change in  $q_0$  was obtained by taking the value of  $q_0$  at the zero-time point (*i.e.* before the enzyme was added) and subtracting the value for  $q_0$  at the experimentally determined time points. The change in  $q_0$  position was always towards lower values of  $q_0$  and thus the value for  $\Delta q_0$  ( $\text{\AA}^{-1}$ ) is always positive. To generate the plots,  $\Delta q_0$  ( $\text{\AA}^{-1}$ ) vs. time (minutes) was plotted, where time is plotted in a log scale. Plotting the FWHM from the analysis above and plotting versus time allowed for the generation of the data Fig. 4b and Fig. S6b. Data was only analyzed from samples where long-range order was still preserved.

## **UV-Vis Enzyme Kinetics**

To 900  $\mu\text{L}$  of 1x PBS in an absorbance cuvette, 25  $\mu\text{L}$  of slow-cooled superlattices were added. While stirring, extinction was monitored at 260- and 520-nm, where a reading was taken every 30 seconds for 30 minutes. Once constant absorbance readings were obtained, 1  $\mu\text{g}$  or 5  $\mu\text{g}$  of RNase A was added to the cuvette while stirring and absorbance readings continued until the extinction values remained constant (30 min total run time).

## **Silica Embedding**

Following slow-cool annealing, the solution phase lattices were transferred to the solid

state *via* silica encapsulation using a modified procedure from that described in Auyeung et al.<sup>6a,6b</sup> 50  $\mu$ L of the slow-cooled samples (eg. lattices containing approximately 50 nM of 10-nm AuNPs) were transferred to a 1.5 mL Eppendorf tube and the volume was raised to 500  $\mu$ L with a solution of 0.5 M NaCl. 1  $\mu$ L of the quaternary ammonium salt, N-trimethoxysilylpropyl-N,N,N-trimethylammonium chloride (TMSPA), was added to the solution of nanoparticle assemblies and the tube was placed on a thermomixer, shaking at 300 rpm at 20 °C. The tube was left shaking for 20 min to allow the TMSPA to electrostatically associate to the negatively-charged phosphate backbone of the DNA and RNA. Subsequently, 2  $\mu$ L of triethoxysilane (TES) was added to the solution to initiate silica growth first around the DNA and RNA where the TMPSA has associated and eventually around the entire lattices. Both the TMSPA and the TES were added in large excess relative to the calculated number of phosphate groups on the DNA and RNA contained in the superlattice samples. The mixture was left on the thermomixer at 20 °C for 24 hours, during which a cloudy precipitate formed above the nanoparticle aggregate that is presumably silica that has undergone bulk precipitation in solution. After 24 hours, the samples were briefly sonicated, then centrifuged at 15000 rpm for 5 s, at which point the solution was removed and filled with 1 mL of DEPC-treated Nanopure water. This process was repeated four times, and after the final removal of the supernatant, the superlattices were re-suspended in 50  $\mu$ L of Nanopure water.

### **Scanning Electron Microscopy (SEM)**

SEM images were obtained at the Northwestern University Atomic and Nanoscale Characterization Experimental Center (NUANCE) on a Hitachi SEM SU8030 instrument at an accelerating voltage of 3 kV. 5  $\mu$ L of solid-state silica embedded lattices in water

were directly drop cast onto a silica wafer (Nova Electronics) that was cut with a diamond scribe (Ted Pella) to a size approximate for imaging.

## References

- (1) Macfarlane, R. J.; Lee, B.; Jones, M. R.; Harris, N.; Schatz, G. C.; Mirkin, C. A. *Science* **2011**, *334*, 204.
- (2) Barnaby, S. N.; Lee, A.; Mirkin, C. A. *Proc Natl Acad Sci U S A* **2014**, *111*, 9739.
- (3) Giljohann, D. A.; Seferos, D. S.; Prigodich, A. E.; Patel, P. C.; Mirkin, C. A. *J. Am. Chem. Soc.* **2009**, *131*, 2072.
- (4) Hurst, S. J.; Lytton-Jean, A. K.; Mirkin, C. A. *Anal Chem* **2006**, *78*, 8313.
- (5) Macfarlane, R. J.; Jones, M. R.; Lee, B.; Auyeung, E.; Mirkin, C. A. *Science* **2013**, *341*, 1222.
- (6) (a) Auyeung, E.; Li, T. I. N. G.; Senesi, A. J.; Schmucker, A. L.; Pals, B. C.; de la Cruz, M. O.; Mirkin, C. A. *Nature* **2014**, *505*, 73; (b) Auyeung, E.; Macfarlane, R. J.; Choi, C. H.; Cutler, J. I.; Mirkin, C. A. *Adv Mater* **2012**, *24*, 5181.